SENSITIVITY ANALYSIS OF A MECHANISTIC HEAT TRANSFER SLUG FLOW MODEL TO THE FREQUENCY

Carlos L. Bassani, langebassani@gmail.com
Fausto A. A. Barbuto, fausto_barbuto@yahoo.ca
Rigoberto E. M. Morales, rmorales@utfpr.edu.br
Multiphase Flow Research Center (NUEM), Federal University of Technology – Paraná (UTFPR), Av. Sete de Setembro, 3165, CEP 80230-901, Curitiba/PR, Brazil

Abstract. *The importance of the slug flow pattern to the oil and gas industry comes from the fact that it occurs over a wide range of gas and liquid flow rates and is therefore frequently found in offshore oil and gas transportation operations. Several experimental works attempted to model some important slug flow parameters such as its frequency and the elongated bubble translational velocity. The experimental correlations that arose from those works are widely used today in mechanistic slug flow simulators so as to provide mathematical closure to the numerical model, as the one that will be presented herein. Yet, those correlations were developed under different experimental conditions, where the pipe geometry, the fluid properties and even the measurement techniques widely affect their performance and their accuracy whenever extrapolations are required. Therefore, this work presents a sensitivity analysis of a heat transfer model for gas-liquid slug flows in horizontal pipes in terms of some slug flow frequency correlations. The sensitivity analysis for the pressure and temperature gradient predictions is shown here, as well as for the mixture heat transfer coefficient and the lengths of the unit cell structures.*

Keywords*: multiphase flow modeling, gas-liquid slug flows, mechanistic approach, heat transfer*

1. NOMENCLATURE

Roman letters

A	Cross sectional area	[m^2]
c	Specific heat	[J/(kg.K)]
D	Diameter	[m]
$freq$	Slug flow frequency	[Hz]
h	Heat transfer coefficient	[W/(m^2.K)]
H	Height	[m]
j	Phase superficial velocity	[m/s]
J	Mixture superficial velocity	[m/s]
k	Thermal conductivity	[W/(m.K)]
K	Head loss coefficient	[-]
L	Length	[m]
$\dot{m}_z$	Scooping mass flow rate	[kg/s]
P	Pressure	[Pa]
R	Phase volumetric fraction	[-]
S	Wetted perimeter	[m]
T	Temperature	[K]
U	Real velocity	[m/s]
z	Pipe axial coordinate	[m]

Greek letters

γ	Pipe inclination	[rad]
κ	Thermal scooping factor	[-]
μ	Viscosity	[Pa.s]
$\xi_{(\%)}$	Defined operator	[%]
$\overline{\xi}$	Defined operator	[-]
ρ	Density	[kg/m^3]
τ	Shear stress	[Pa]

Indexes

B	Bubble region
ext	External medium
i	Gas-water interface
in	Pipe inlet
G	Gas
L	Liquid
m	Mixture
n	Node index
$ov.$	Overall
S	Slug region
T	Unit cell translation
U	Unit cell
W	Wall
ε	Refers to a generic parameter of the slug flow
ϕ	Refers to the phase $(\phi = L;G)$
ψ	Refers to the unit cell region $(\psi = B;S)$
$\phi\psi$	Refers to the unit cell structure $(\phi\psi = LB; LS; GB; GS$.

2. INTRODUCTION

Over 90% of the oil and gas produced in Brazil come from offshore operations (ANP, 2015), that is, from submarine wells. The oil and gas produced by this kind of operation is typically accompanied by water (brine) and sand, and the mixture usually flows in the slug flow pattern. Slug flows are characterized by the intermittent passage of elongated bubbles, flowing over a liquid film; and liquid slugs, which may contain dispersed bubbles in their interior (Shoham, 2006). Together, these structures form the so-called *unit cell*.

Several approaches have been used to model slug flows, namely: stationary or quasi-stationary mechanistic models (Bassani et al., 2016b; Cook and Behnia, 2000; Shoham, 2006; Taitel and Barnea, 1990), Eulerian transient drift flux models (Danielson, 2011; Zerpa et al., 2013), Eulerian transient two-fluid models (Issa and Kempf, 2003; Simões et al., 2014), Lagrangian transient slug tracking models (Medina et al., 2015; Nydal and Banerjee, 1996; Taitel and Barnea, 1998) and hybrid models (Kjeldby et al., 2013). Few studies consider the heat transfer between the mixture – which comes from the well as a moderately hot stream – and the cold external medium, the deep ocean waters (Bassani et al., 2016b; Medina et al., 2015; Simões et al., 2014; Zerpa et al., 2013).

Regardless the approach used for modeling slug flows, to a greater or lesser degree, it depends on some kind of closure relationship obtained from experimental data. Thus, many authors developed closure relationships based on experimental data, notably for the bubble nose translational velocity (Bendiksen, 1984; Petalas and Aziz, 1998), for the slug flow frequency (Heywood and Richardson, 1979; Schulkes, 2011) and for the gas fraction in the slug region (Andreussi et al., 1993; Barnea and Brauner, 1985). In particular, high discrepancies between the different correlations for the slug flow frequency were reported in the literature (Antunes et al., 2014), raising concerns within the scientific community on whether their application is valid as closure to the aforementioned slug flow models.

In this sense, the present work analyzes the sensitivity of the slug flow hydrodynamics and heat transfer in terms of the slug flow frequency chosen for a mechanistic model (Bassani et al., 2016b). The methodology herein presented follows the one proposed in a previous work for the sensitivity analysis of the same model in terms of a selected unit cell translational velocity correlation (Bassani et al., 2015). The analyzed parameters are the pressure and temperature gradients, the mixture heat transfer coefficient and the lengths of unit cell regions.

3. MATHEMATICAL MODEL

The problem consists in characterizing gas-liquid slug flows with heat transfer in horizontal pipelines. The slug flow is characterized by the intermittent passage of *unit cells* (Fig. 1a). A unit cell is composed by two defined *regions* ψ, the slug (*S*) and the elongated bubble (*B*). Both regions may contain each *phase* ϕ, that is, the gas (*G*) or the liquid (*L*). Each phase inside each region is called a *unit cell structure* $\phi\psi$.

The quasi-stationary mechanistic model herein used (Bassani et al., 2016a) is based on an *Upwind Differencing Scheme*, with the pipeline divided in nodes spaced by Δz (Fig. 1b). The superficial velocities of the phases (j_ϕ) and the mixture pressure (*P*) and temperature (*T*) are considered known at the pipe inlet. The thermal boundary condition is an external medium with constant temperature (T_{ext}) and constant heat transfer coefficient (h_{ext}) – the ocean waters. A unit cell geometry model (Taitel and Barnea, 1990) is used for characterizing the elongated bubble profile and the unit cell region lengths and phase fractions. The mass balance is based on the volumetric phase fractions and is applied in the determination of the velocities of the unit cell structures. The velocities of those structures allow finding: (i) the structures' shear stresses used in the evaluation of the pressure drop in terms of the momentum balance; and (ii) the structures' heat transfer coefficient, used in the evaluation of the temperature drop in terms of the energy balance. Knowing the pressure and temperature drop, the gas superficial velocity can be recalculated node after node, whereas the liquid one is assumed constant due to the presumed incompressibility of this phase. The process is repeated until the end of the pipeline is reached.

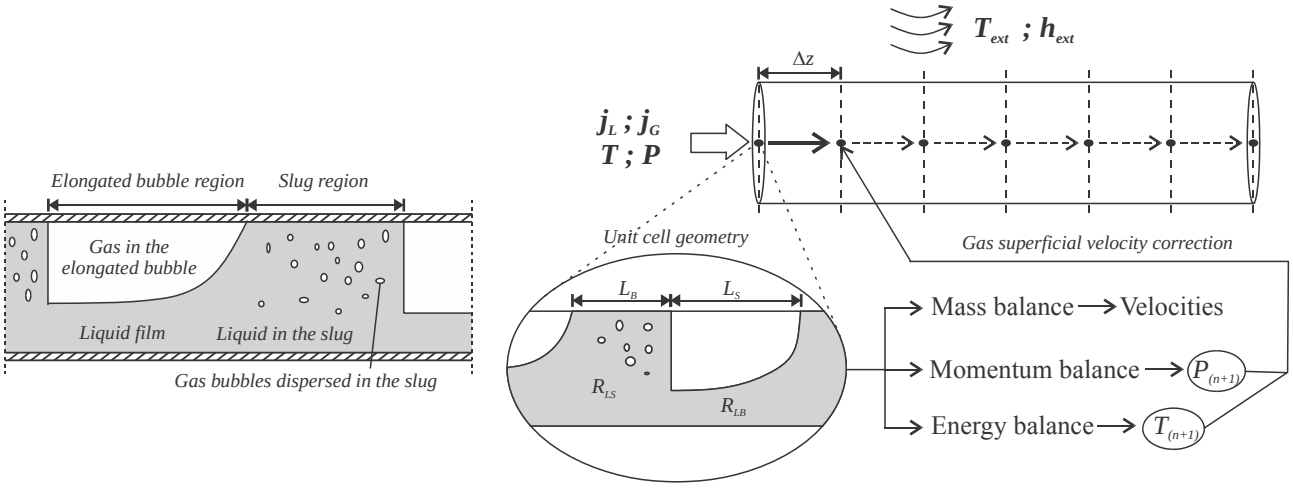

Figure 1. a) Unit cell definition and b) problem characterization.

The main assumptions of the model are: (i) one-dimensional and horizontal flow; (ii) incompressible liquid and ideal gas; (iii) Newtonian fluids; (iv) quasi-stationary mechanistic approach, (v) uniform velocity profile and constant phase fractions in each unit cell structure; (vi) constant external medium temperature as boundary condition; (vii) negligible gas energy; (viii) negligible kinetic energy; (ix) no mass transfer.

The liquid and gas mass balance is applied to the control volume of Fig. 2a, which moves forward with the unit cell translational velocity U_T, leading to an expression for the velocities of the phases in the elongated bubble region (Taitel and Barnea, 1990):

$$U_{LB} = U_T - \left(U_T - U_{LS}\right)\frac{R_{LS}}{R_{LB}} \quad ; \quad U_{GB} = U_T - \left(U_T - U_{GS}\right)\frac{\left(1-R_{LS}\right)}{R_{GB}} \tag{1}$$

where $R_{\phi\psi}$ is the phase fraction in the unit cell region and $U_{\phi\psi}$ is the velocity of the unit cell structures. The dispersed bubbles velocity is considered equal to the slug one, $U_{GS} \approx U_{LS}$, an assumption valid for horizontal flows (Harmathy, 1960). Therefore, the slug velocity is approximately equal to the mixture superficial velocity when considering a constant mixture velocity along the unit cell (Shoham, 2006), that is, $U_{LS} \approx J$.

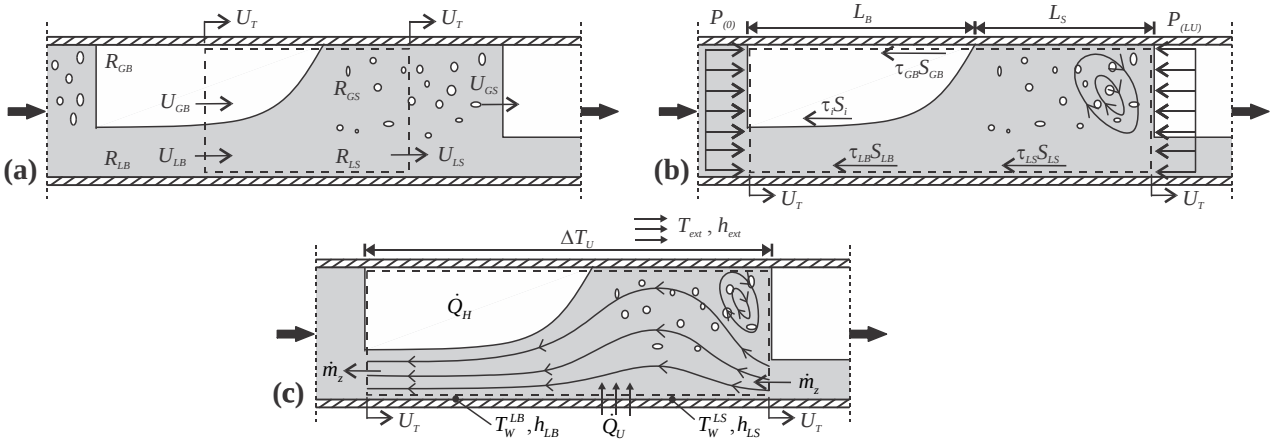

Figure 2. Control volume definitions for: a) mass, b) momentum and c) energy balances.

The unit cell geometry is estimated using Taitel and Barnea's (1990) model. A mixed momentum balance between the gas and the liquid is applied to the elongated bubble region to find an ODE for the film height H_{LB}

$$\frac{dH_{LB}}{dz} = \frac{\dfrac{\tau_{LB}S_{LB}}{A_{LB}} - \dfrac{\tau_{GB}S_{GB}}{A_{GB}} - \tau_i S_i\left(\dfrac{1}{A_{LB}} + \dfrac{1}{A_{GB}}\right) + \left(\rho_L - \rho_G\right)g\sin\gamma}{\left(\rho_L - \rho_G\right)g\cos\gamma - \left(\rho_L \dfrac{\left|U_{LB} - U_T\right|\left(U_{LB} - U_T\right)}{R_{LB}} + \rho_G \dfrac{\left|U_{GB} - U_T\right|\left(U_{GB} - U_T\right)}{R_{GB}}\right)\dfrac{dR_{LB}}{dH_{LB}}} \tag{2}$$

where z is the pipeline axial coordinate, $\tau_{\phi\psi}$ is the shear stress of the unit cell structure, $A_{\phi\psi}$ is the cross sectional area occupied by the unit cell structure, $S_{\phi\psi}$ is the structure wetted perimeter, γ is the pipeline inclination and g is the gravitational acceleration. Equation (2) is a function of the film height only and can be numerically integrated over the elongated bubble length until convergence with the liquid mass balance in the unit cell is achieved:

$$\frac{L_U\left(U_{LS}R_{LS} - j_L\right)}{U_T} = L_B\left(R_{GB} - R_{GS}\right) \tag{3}$$

The bubble length is mathematically determined as an integral over all the infinitesimal dz integration steps, $L_B = \int_0^{L_B} dz$. The gas fraction in the bubble is then calculated as $R_{GB} = 1 - \frac{1}{D}\int_0^{L_B} \frac{dH_{LB}}{dz} dz$. The unit cell length L_U is determined by the ratio between the unit cell translational velocity and the slug flow frequency, $L_U = U_T / freq$. The slug length L_S is then straightforwardly obtained, $L_S = L_U - L_B$.

Knowing the unit cell geometry and the structures velocities, Eqs. (1) to (3), the pressure distribution along the pipeline can be determined by applying the momentum balance to the control volume of Fig. 2b:

$$P_{(n)} = P_{(n+1)} - \left[\underbrace{\frac{\tau_{LS} S_{LS}}{A} \frac{L_S}{L_U}}_{slug} + \underbrace{\frac{\left(\tau_{LB} S_{LB} + \tau_{GB} S_{GB} + \tau_i S_i\right)}{A} \frac{L_B}{L_U}}_{elongated\ bubble} + \underbrace{K \rho_L \frac{\left(U_{LB} - U_T\right)^2}{2 L_U}}_{wake\ zone} \right] \Delta z \tag{4}$$

where (*n*) stands for the current node and (*n+1*) its consecutive one, Δz is the nodal spacing and L_ψ is the length of the unit cell region. The pressure distribution is a function of: (i) the slug friction with the wall (the interfacial friction between the dispersed bubble and the liquid continuous phase is neglected); (ii) the elongated bubble friction (that is, the friction between film/wall, gas elongated bubble/wall and in the gas-water interface); and (iii) the head loss due to the recirculation at the rear of the elongated bubble, also called *wake zone*, here modeled as a sudden expansion of the liquid-filled cross sectional area (Cook and Behnia, 2000), characterized by head loss coefficient $K \approx 0.4$ (Bassani et al., 2016b).

An expression for the mixture temperature variation along the pipeline is obtained by applying the energy conservation equation to the control volume of Fig. 2c:

$$T_{(n+1)} = T_W + \left(T_{(n+1)} - T_W\right) \exp\left(- \left[\frac{\overbrace{h_{LB} S_{LB} L_B}^{film} + \overbrace{h_{LS} S_{LS} L_S}^{slug} - \overbrace{\kappa \dot{m}_z c_L}^{scooping}}{\rho_L R_{LU} A U_T L_U c_L} \right] \Delta z \right) \tag{5}$$

where T_W is the wall temperature, $h_{\phi\psi}$ is the heat transfer coefficient of the unit cell structure and ρ_L and c_L are the liquid density and specific heat, respectively. Equation (5) takes the following points into account: (i) the convection heat transfer in the slug and in the film, separately; and (ii) the heat transfer between two consecutive unit cells, also known as *thermal scooping phenomenon* (Bassani et al., 2016b). The scooping phenomenon is defined by the thermal scooping factor κ, Eq. (6), and the scooping mass flow rate $\dot{m}_z$, Eq. (7). The mean liquid fraction in the unit cell R_{LU} is weighed by the unit cell region lengths, Eq. (8). The link between the wall temperature T_W and the external medium one T_{ext} – that is, the thermal boundary condition – is established by Eq (9), using the overall heat transfer coefficient concept, $h_{\phi\psi}^{ov.}$, Eq. (10). With the knowledge of both temperature and pressure in the consecutive node (*n+1*), the gas superficial velocity can be corrected by Eq. (11). The heat transfer coefficient h_m is then estimated by Eq. (12). Equations (6) to (12) are summarized in Tab. 1.

Table 1. Auxiliary equations for the energy balance.

Description	***Equations***	***Ref.***
Scooping phenomenon parameters (Bassani et al., 2016b)	$\kappa = \exp\left(\frac{h_{LB} S_{LB} L_B}{\rho_L c_L A R_{LB} U_{LB}}\right) - \exp\left(-\frac{h_{LS} S_{LS} L_S}{\rho_L c_L R_{LS} A U_{LS}}\right) \quad \dot{m}_z = \rho_L R_{LB} A\left(U_T - U_{LB}\right) = \rho_L R_{LS} A\left(U_T - U_{LS}\right)$	(6),(7)
Weighed liquid fraction	$R_{LU} = \left(R_{LS} L_S + R_{LB} L_B\right) / L_U$	(8)
Wall temperature	$T_W = T + \left[\frac{h_{LB}^{ov.}}{h_{LB}} \frac{L_B}{L_U} + \frac{h_{LS}^{ov.}}{h_{LS}} \frac{L_S}{L_U}\right] \frac{D}{D_{ext}} \left(T_{ext} - T\right) \quad h_{\phi\psi}^{ov.} = \left[\frac{D}{D_{ext} h_{ext}} + \frac{D \ln\left(D_{ext}/D\right)}{2 k_{eq}} + \frac{1}{h_{\phi\psi}}\right]^{-1}$	(9),(10)
Gas superficial velocity correction	$j_{G(n)} = j_{G(n-1)} \frac{P_{(n-1)}}{P_{(n)}} \frac{T_{(n)}}{T_{(n-1)}}$	(11)
Mixture heat transfer coefficient	$h_m = \left(h_{LB} \frac{S_{LB}}{S} \frac{L_B}{L_U} + h_{LS} \frac{S_{LS}}{S} \frac{L_S}{L_U} - \frac{\kappa \dot{m}_z c_L}{S L_U}\right) \frac{j_L}{R_{LU} U_T}$	(12)

4. CLOSURE RELATIONSHIPS AND SOLUTION METHOD

Variables outnumber equations in the mechanistic model presented in the previous section. Therefore, it is usual to evaluate some parameters by experimental correlations. In the present work, the unit cell translational velocity U_T will be calculated as proposed by Petalas and Aziz (1998), whereas the gas fraction in the slug body R_{GS} will be evaluated as Andreussi et al. (1993). The slug flow frequency will be evaluated by six different correlations found in the literature and presented in Tab. 2, keeping in mind that the purpose of the work is to understand the effects brought to the slug

flow hydrodynamics and heat transfer by the choice between these correlations. All the correlations in Tab. 2 are valid for the input data ranges simulated in the present work.

The model was implemented as a procedural *Fortran90* code. An *Upwind Differencing Scheme* was used, following the stencil presented in Fig. 1b. The friction factors and the heat transfer coefficients of the unit cell structures are evaluated by the Blasius and Gnielinski correlations respectively (apud Incropera et al., 2007).

Table 2. Closure relationships for the slug flow frequency.

Author(s)	*Frequency correlation*	*Inclination*
Gregory and Scott (1969)	$freq = 0.0226\left[\frac{j_L}{gD}\left(\frac{19.75}{J}+J\right)\right]^{1.2}$	Horizontal
Heywood and Richardson (1979)	$freq = 0.0434\left[\lambda\left(\frac{2.02}{D}+Fr_m\right)\right]^{1.02}$ $Fr_m=\frac{J^2}{gD}$	Horizontal
Nydal (1991)	$freq = 0.088\frac{\left(1.5+j_L\right)^2}{gD}$	Horizontal
Cai et al. (1999)	$freq = 0.018\mathrm{e}^{\sin\gamma}\left[\frac{j_L}{gD}\left(\frac{36}{V_t}+V_t\right)\right]^{1.2}$ $V_t=1.25J$	Horizontal to vertical
Zabaras (2000)	$freq = \left[0.836+2.75\left(\sin\gamma\right)^{0.25}\right]0.0226\left[\frac{j_L}{gD}\left(\frac{19.75}{J}+J\right)\right]^{1.2}$	Horizontal to vertical
Schulkes (2011)	$freq=\frac{J}{D}\Psi_{(\lambda)}\Phi_{(\mathrm{Re}_L)}\Theta_{(\gamma,Fr_L)}$ $\Psi_{(\lambda)}=0.016\lambda\left(2+3\lambda\right)$ $\lambda=\frac{j_L}{J}$ $\Phi_{(\mathrm{Re}_L)}=\begin{cases}12.1\mathrm{Re}_L^{-0.37}, & for\ \mathrm{Re}_L<4000\\ 1, & for\ \mathrm{Re}_L\geq 4000\end{cases}$ $\mathrm{Re}_L=\frac{\rho_L j_L D}{\mu_L}$ $\Theta_{(\gamma,Fr_L)}=\begin{cases}1+\frac{2}{Fr_L}\mathrm{sgn}\left(\gamma\right)\sqrt{\lvert\gamma\rvert}, & for\ \lvert\gamma\rvert\leq 0.17\\ \frac{1.8}{Fr_L}\left(0.6+2\gamma-\gamma^2\right), & for\ \gamma>0.17\end{cases}$ $Fr_L=\frac{j_L}{\sqrt{Dg\cos\gamma}}$	Horizontal to vertical

5. SENSITIVITY ANALYSIS

Yet all the slug flow frequency correlations presented in Tab. 2 are valid for the cases that will be simulated, their results differ due to the experimental techniques and methodologies applied to each study. The aim of the sensitivity analysis herein presented is to understand the propagation of uncertainties introduced by different slug flow frequency correlations chosen to supply closure to the mechanistic model. This uncertainty will propagate during the simulation. The question to be answered is how the model responds to this uncertainty propagation. What are the sensitive and the non-sensitive parameters in the model? Based on the answers to those questions, this work aims at demystifying the 'concerns' that part of the scientific community feels towards the application of the slug flow frequency as a valid closure correlation to this kind of model.

Two operators need to be defined prior to the sensitivity analysis. The first one, Eq. (13), is the amplitude percent range of a generic parameter ε between the simulations carried out for any of the *i* slug flow frequency correlations. The second one, Eq. (14), is the normalization of $\xi\varepsilon_{(\%)}$ in terms of the amplitude percent range for different frequency correlations, $\xi\, freq_{(\%)}$.

$$\xi\varepsilon_{(\%)}=\frac{\max\left(\varepsilon_i\right)-\min\left(\varepsilon_i\right)}{\mathrm{mean}\left(\varepsilon_i\right)}\times\left(100\%\right) \tag{13}$$

$$\overline{\xi}\varepsilon=\frac{\xi\varepsilon_{(\%)}}{\xi\, freq_{(\%)}} \tag{14}$$

The operator $\overline{\xi}\varepsilon$ represents the amplification or damping of the amplitude percent range of a generic parameter ε between the simulations using any of the the *i* different closure relationships in comparison to the amplitude percent range of these frequency closure relationships. Therefore, when $\overline{\xi}\varepsilon\approx 1$, the uncertainties on choosing the different frequency correlations propagate linearly to the parameter ε. For $\overline{\xi}\varepsilon\gg 1$, there is amplification of the uncertainties, showing that the parameter ε is sensitive to the imposed frequency correlation. For $\overline{\xi}\varepsilon\ll 1$, there is damping of the

uncertainties, showing that the parameter ε is not sensitive to the imposed frequency correlation. The degree of sensitivity is related to absolute value of $\overline{\xi}\varepsilon$.

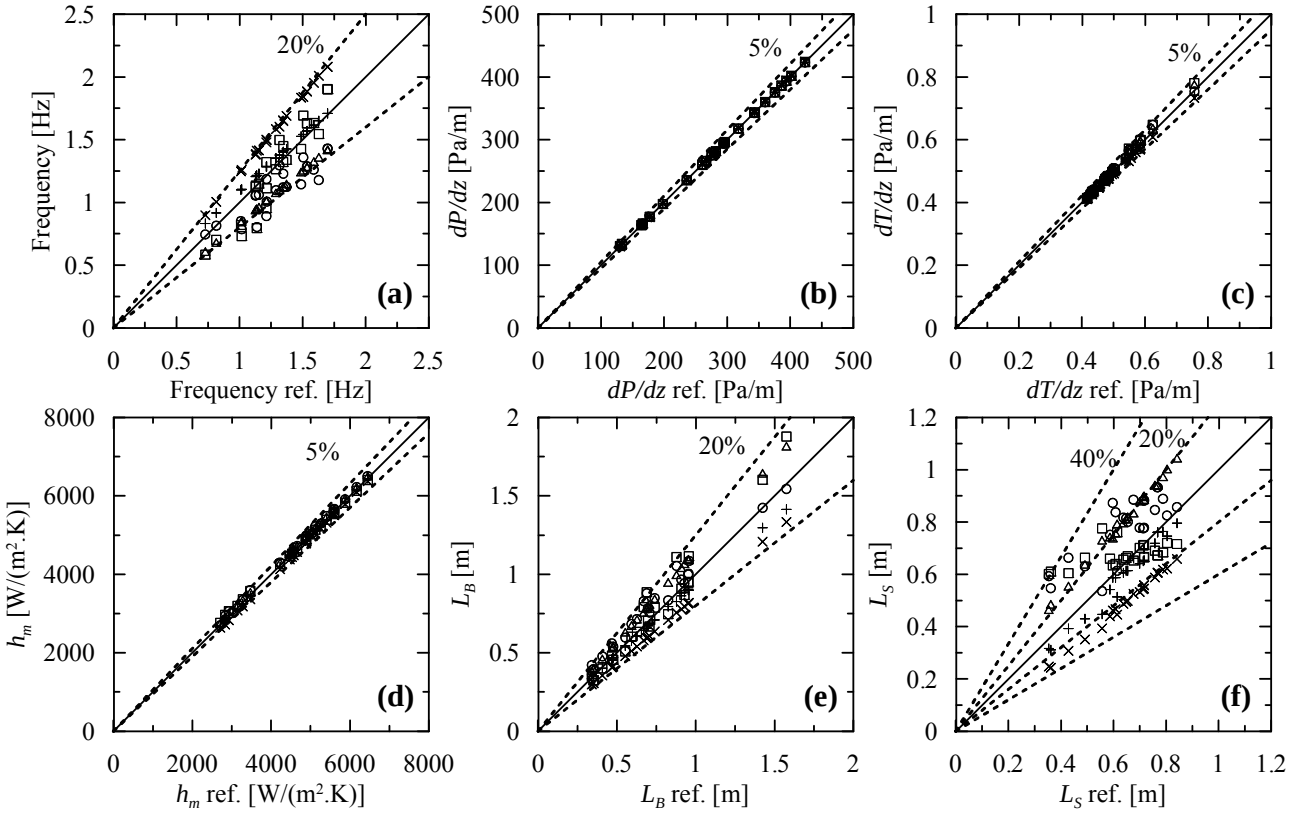

Figure 3. Sensitivity analysis for (+ Heywood and Richardson, 1979; ○ Nydal, 1991; × Cai et al., 1999; ▵ Zabaras, 2000; □ Schulkes, 2011): a) slug flow frequency, b) pressure gradient, c) temperature gradient, d) mixture heat transfer coefficient, e) elongated bubble length and f) slug length.

The simulations reproduce the experimental measurements of Lima (2009) for an air-water flowing through a 52-mm ID copper pipe with 1-mm wall width. The mixture is cooled by the water flowing co-currently through a concentric annular space, similarly to a pipe-and-shell heat exchanger. The experimental measurements cover the following ranges: $0.58 \le j_L \le 1.93$ m/s, $0.22 \le j_G \le 0.79$ m/s, $135.7 \le P_{in} \le 182.2$ kPa, $283.1 \le T_{ext} \le 288.1$ K, $307.7 \le T_{in} \le 318.7$ K and $1525 \le h_{ext} \le 2620$ W/(m^2.K). Twenty-four (24) inlet conditions and the six slug flow frequency correlations in Tab. 2 were used in the simulations, totalling 144 runs.

Figure 3 presents the comparison between the results obtained with each slug flow frequency correlation. The simulation using Gregory and Scott (1969) correlation was used as the reference for the x-axis. It is important to notice that Fig. 3 represents a comparison between simulations using different frequency closure correlations only. The model comparison with experimental data has already been presented in the original work (Bassani et al., 2016b).

Figure 3a shows that the slug flow frequency correlations present a ±20% discrepancy between themselves. This represents, approximately, a 40% amplitude percent range between the frequency correlations for the range of the simulations – with a respective $\xi freq_{(\%)}$ average and maximum values of 42.6 and 58.3%. The pressure and temperature gradients and the mixture heat transfer coefficient are practically non-sensitive to the selected slug flow frequency correlation, with $\overline{\xi}$ below 0.16, with the results staying within a ±5% range (Figs. 3b-d). The unit cell region lengths are more sensitive to the selected frequency correlation. The elongated bubble length propagates the uncertainties as an almost linear trend, staying within a range of ±20% (Fig. 3e) and with an average $\overline{\xi} L_B$ = 0.55. The slug length is the most sensitive parameter here evaluated, where the percent range is amplified to ±40% (Fig. 3f), with an average and maximum $\overline{\xi} L_S$ of 0.98 and 1.56, respectively.

Table 3 summarizes the sensitivity analysis using the operators $\xi_{(\%)}$ and $\overline{\xi}$.

Table 3. Sensitive analysis using the operators $\xi_{(\%)}$ and $\overline{\xi}$.

$\xi\varepsilon_{(\%)}\left(\overline{\xi}\varepsilon\right)$	*freq*	*dP/dz*	*dT/dz*	h_m	L_B	L_S
Average	42.6	0.4 (0.01)	3.3 (0.06)	3.9 (0.07)	30.1 (0.55)	54.1 (0.98)
Standard deviation	6.2	0.3 (0.01)	1.7 (0.03)	1.7 (0.03)	3.7 (0.07)	11.9 (0.22)
Maximum	58.3	1.5 (0.03)	7.4 (0.13)	8.7 (0.16)	39.2 (0.71)	86.1 (1.56)
Minimum	36.9	≈ 0 (≈ 0)	1.3 (0.02)	2.1 (0.04)	25.6 (0.47)	42.9 (0.78)

6. CONCLUSIONS

An analysis of a mechanistic model for predicting gas-liquid horizontal slug flows with heat transfer aimed at gauging the sensitivity of the model to slug flow frequency correlations used as model closure was conducted. The six different slug flow frequency correlations found in the literature – all valid for the simulation cases – differ from each other by approximately ±20%. The uncertainty imposed by the frequency correlation chosen to provide closure to the model propagated during the simulation. The pressure and temperature gradients and the mixture heat transfer are not sensitive to the selected slug flow frequency correlation, whereas the unit cell region lengths are. Therefore, one can conclude that the reliability on predicting the unit cell geometry of slug flows might be a concern whenever using a mechanistic model based on frequency correlations. On the other hand, temperature and pressure distributions can be quite well predicted by this kind of approach.

7. ACKNOWLEDGEMENTS

The authors acknowledge the financial support of ANP and FINEP through the Human Resources Program for Oil and Gas Segment PRH-ANP (PRH 10-UTFPR), TE/CENPES/PETROBRAS (0050.0068718.11.9) and the National Council for Scientific and Technological Development (CNPq).

8. REFERENCES

Andreussi, P., Bendiksen, K.H., Nydal, O.J., 1993. Void distribution in slug flow. Int. J. Multiph. Flow 19, 817–828. doi:10.1016/0301-9322(93)90045-V

ANP, 2015. Anuário Estatístico Brasileiro do Petróleo, Gás Natural e Biocombustíveis 2015. Disponible at: http://www.anp.gov.br/?pg=76798&m=&t1=&t2=&t3=&t4=&ar=&ps=&1447767577660.

Antunes, M.M., Cozin, C., Barbuto, F.A.A., Morales, R.E.M., Rodrigues, H.T., 2014. Analysis of Slug Frequency Correlations for Two-Phase Gas-Liquid Horizontal Slug Flow, in: 4th Joint US-European Fluids Engineering Division Summer Meeting Collocated with the ASME 2014 12th International Conference on Nanochannels, Microchannels, and Minichannels. Chicago.

Barnea, D., Brauner, N., 1985. Holdup of the liquid slug in two phase intermittent flow. Int. J. Multiph. Flow. doi:10.1016/0301-9322(85)90004-7

Bassani, C.L., Barbuto, F.A.A., Morales, R.E.M., Sum, A.K., 2016a. An analysis of the coupled effects of mass transfer, slug flow hydrodynamics and heat transfer during hydrate formation using a quasi-stationary mechanistic model, in: Submitted at 10th North American Conference on Multiphase Technology. BHR Group, Banff/Canada.

Bassani, C.L., Pereira, F.H.G., Barbuto, F.A.A., Morales, R.E.M., 2016b. Modeling the scooping phenomenon for the heat transfer in liquid-gas horizontal slug flows. Appl. Therm. Eng. 98, 862–871. doi:10.1016/j.applthermaleng.2015.12.104

Bassani, C.L., Pereira, F.H.G., Barbuto, F.A.A., Morales, R.E.M., 2015. Sensitivity analysis of a horizontal stationary heat transfer slug flow model on the elongated bubble velocity, in: 23rd ABCM International Congress of Mechanical Engineering. Rio de Janeiro, Brazil.

Bendiksen, K.H., 1984. An experimental investigation of the motion of long bubbles in inclined tubes. Int. J. Multiph. Flow 10, 467–483.

Cai, J.Y., Wang, H.W., Hong, T., Jepson, W.P., 1999. Slug frequency and length inclined large diameter multiphase pipeline, in: 4th Multiphase Flow and Heat Transfer International Symposium. Xi'an, China.

Cook, M., Behnia, M., 2000. Pressure drop calculation and modelling of inclined intermittent gas-liquid flow. Chem. Eng. Sci. 55, 4699–4708. doi:10.1016/S0009-2509(00)00065-8

Danielson, T., 2011. A simple model for hydrodynamic slug flow, in: Offshore Technology Conference. Offshore Technology Conference, Houston/TX, USA. doi:10.4043/21255-MS

Gregory, G.A., Scott, D.S., 1969. Correlation of liquid slug velocity and frequency in horizontal cocurrent gas-liquid slug flow. AIChE J. 15, 933–935. doi:10.1002/aic.690150623

Harmathy, T.Z., 1960. Velocity of large drops and bubbles in media of infinite or restricted extent. AIChE J. 6, 281–288. doi:10.1002/aic.690060222

Heywood, N.I., Richardson, J.F., 1979. Slug flow of air-water mixtures in a horizontal pipe: Determination of liquid

holdup by γ-ray absorption. Chem. Eng. Sci. doi:10.1016/0009-2509(79)85174-X
Incropera, F.P., DeWitt, D.P., Bergman, T.L., Lavine, A.S., 2007. Fundamentals of Heat and Mass Transfer, Water. doi:10.1016/j.applthermaleng.2011.03.022
Issa, R.I., Kempf, M.H.W., 2003. Simulation of slug flow in horizontal and nearly horizontal pipes with the two-fluid model. Int. J. Multiph. Flow 29, 69–95. doi:10.1016/s0301-9322(02)00127-1
Kjeldby, T.K., Henkes, R. a W.M., Nydal, O.J., 2013. Lagrangian slug flow modeling and sensitivity on hydrodynamic slug initiation methods in a severe slugging case. Int. J. Multiph. Flow 53, 29–39. doi:10.1016/j.ijmultiphaseflow.2013.01.002
Lima, I.N.R.C., 2009. Estudo Experimental da Transferência de Calor no Escoamento Bifásico Intermitente Horizontal. Master Thesis, University of Campinas, Campinas, Brazil.
Medina, C.D.P., Bassani, C.L., Cozin, C., Barbuto, F.A.A., Junqueira, S.L.M., Morales, R.E.M., 2015. Numerical simulation of the heat transfer in fully developed horizontal two-phase slug flows using a slug tracking method. Int. J. Therm. Sci. 88, 258–266. doi:10.1016/j.ijthermalsci.2014.05.007
Nydal, O.J., 1991. An experimental investigation of slug flow. PhD Thesis, University of Oslo, Oslo, Norway.
Nydal, O.J., Banerjee, S., 1996. Dynamic slug tracking simulations for gas-liquid flow in pipelines. Chem. Eng. Commun. 141, 13–39. doi:10.1080/00986449608936408
Petalas, N., Aziz, K., 1998. A mechanistic model for multiphase flow in pipes, in: Annual Technical Meeting. Petroleum Society of Canada, Calgary, Canada. doi:10.2118/98-39
Schulkes, R., 2011. Slug frequencies revisited, in: 15th International Conference on Multiphase Production Technology. BHR Group, Cannes, France, pp. 311–325.
Shoham, O., 2006. Mechanistic modeling of gas-liquid two-phase flow in pipes, 1st ed. Society of Petroleum Engineers, Richardson, USA.
Simões, E.F., Carneiro, J.N.E., Nieckele, A.O., 2014. Numerical prediction of non-boiling heat transfer in horizontal stratified and slug flow by the two-fluid model. Int. J. Heat Fluid Flow 47, 135–145. doi:10.1016/j.ijheatfluidflow.2014.03.005
Taitel, Y., Barnea, D., 1998. Effect of gas compressibility on a slug tracking model. Chem. Eng. Sci. 53, 2089–2097. doi:10.1016/S0009-2509(98)00007-4
Taitel, Y., Barnea, D., 1990. A consistent approach for calculating pressure drop in inclined slug flow. Chem. Eng. Sci. 45, 1199–1206. doi:10.1016/0009-2509(90)87113-7
Zabaras, G.J., 2000. Prediction of Slug Frequency for Gas/Liquid Flows. SPE J. 5 (3), 252–258. doi:10.2118/65093-PA
Zerpa, L.E., Rao, I., Aman, Z.M., Danielson, T.J., Koh, C.A., Sloan, E.D., Sum, A.K., 2013. Multiphase flow modeling of gas hydrates with a simple hydrodynamic slug flow model. Chem. Eng. Sci. 99, 298–304. doi:10.1016/j.ces.2013.06.016

9. RESPONSIBILITY NOTICE

The authors are the only responsible for the printed material included in this paper.